DESIGN OPTIMISATION FOR OPTICALLY TRACKED POINTERS

B. De Coninck[1], J. Victor[2], P. De Baets[3], S. Herregodts[2] and M.A. Verstraete[2]

[1] Ghent University, Belgium
[2] Ghent University, Department of Physical Medicine and Orthopaedic Surgery, Belgium
[3] Ghent University, Laboratory Soete, Belgium

Abstract: The use of mechanical pointers in optical tracking systems is needed to aid registration processes of unlocated rigid bodies. Error on the target point of a pointer can cause wrong positioning of vital objects and as such these errors have to be avoided. In this paper, the different errors that originate during this process are described, after which this error analysis is used for the optimisation of an improved pointer design. The final design contains six coplanar fiducials, favored by its robustness and low error. This configuration of fiducials is then analysed theoretically as well as practically to understand how it is performing. The error on tracking the target point of the pointer is found with simulation to be around 0.7 times the error of measuring one fiducial in space. However, practically this error is about equal to the fiducial tracking error, due to the non-normally distributed errors on each separate fiducial.

Keywords: Optical tracking; pointer; optimisation; fiducial position

1 INTRODUCTION

An optical tracking system is often used to trace the movement of rigid bodies in 3D space. Infrared cameras are therefore placed around the setup, which can track the motion of reflective fiducials. These are rigidly connected to the rigid bodies that need to be followed in 3D space. Mostly, the shape of the rigid body is known with a certain accuracy but the relative position between the fiducials and this body is unknown. This is where pointers are used, namely to register the location of points on the rigid body with the pointer tip. A pointer is the combination of several fiducials. These are positioned in a fixed configuration around a pointer tip, which is the target point during the usage of the pointer. By performing a calibration process of the pointer, the relative position between the different fiducials and the pointer tip is found. When the fiducials of the pointer are then tracked, the known shape of the configuration of the pointer fiducials is matched in this cloud and the pointertip position is calculated. The position of the pointer tip with respect to the fixed markerset of the rigid body is thus known, after which a matching procedure matches the rigid body shape in this point cloud to find the total configuration. This method is presented in a flowchart in figure 1.

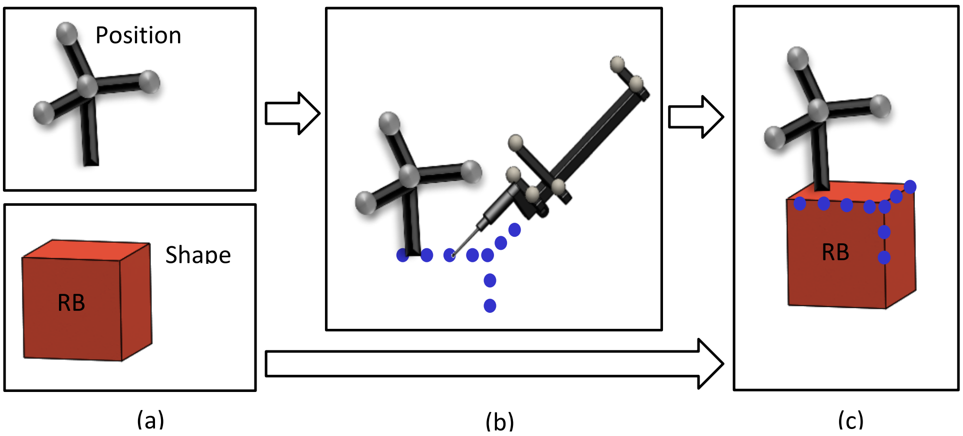

Figure 1: Flowchart of registration process: (a) 2 inputs, the position of the markerset – which is fixed to the rigid body - tracked by the optical tracking system and the shape of the rigid body. (b) Moving with the pointer over the surface of the rigid body to obtain points of the rigid body with respect to the fixed makerset. (c) Known positioning between the markerset and the rigid body.

When a tracking system, containing cameras and a traceable collection of fiducials – for instance a pointer - , is analysed, several types of errors can be defined. Each camera has a 2D view and therefore an associated 2D positioning error in this observed plane. This error is called the image plain error (IPE). By combining this for the present cameras, to go to a 3D positioning system, the errors are also combined into a fiducial localisation error (FLE). This can physically be described as the 3D distance between the actual position of a fiducial and the measured one, as pictured in figure 2.a. Because the FLE can be measured directly from the usage of the camera system and this error is linked with the errors in subsequent steps, the starting point of this paper will be the FLE.

Other types of errors are introduced when several fiducials are combined in a fixed relative position, with the pointer as main example. The real design of fiducials on the pointer is known with a certain accuracy due to the production process or a calibration process. Then the tracking system matches this known shape in the measured positions of the fiducial markers, but because of the error on each measurement of a fiducial, this matching process also has an inaccuracy. The fiducial registration error (FRE) is then the residual distance between the calculated and measured positions after the matching process. This error is shown in figure 2.b. A last error introduces itself if the position of other points than the fiducial markers is to be known. This error can be calculated if the known 3D spot with respect to the markerset is known, which is then used after the alignment. This error is called the target registration error (TRE) and is of major importance for the pointer. The arrow in Figure 2.c shows this error.

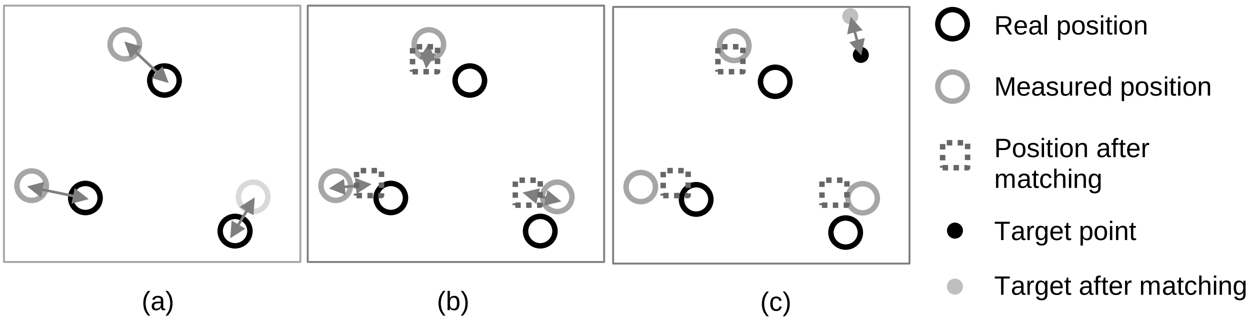

Figure 2: kind of errors for an optical tracking system: (a) FLE for each fiducial. (b) FRE at the fiducial positions after the matching procedure. (c) TRE at the target after the matching procedure.

M. Fitzpatrick et al. [1] derived functions between the different kinds of errors to link these with each other. For this research, the major formula is the one that describes the TRE in function of the FLE:

$$\langle TRE^2(r)\rangle \approx \frac{\langle FLE^2\rangle}{N}\cdot\left(1+\frac{1}{3}\cdot\sum_{k=1}^{3}\frac{d_k^2}{f_k^2}\right) \tag{1}$$

$$f_k = \sqrt{f_{k,1}^2 + f_{k,2}^2 + \dots + f_{k,n}^2} \tag{2}$$

With $\langle\cdot\rangle$ the symbol of mean value, N the number of fiducials, d_k the distance from the target point to the k-th principal axes of the collection of fiducials at the pointer and f_k the root mean square distance of the different fiducials to the same principal axes. This formula only holds true when the x-, y-, and z-coordinates of the fiducial measurements are normally distributed. Moreover, it is an approximation because higher order terms are neglected in the derivation. The different parameters are plotted and explained in figure 3.

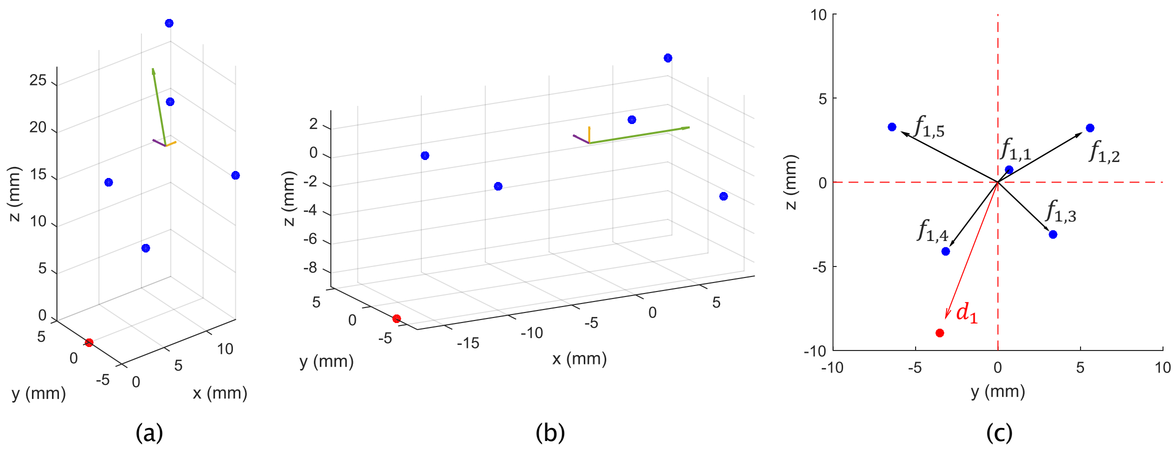

Figure 3: Explanation of formula (1): (a) Starting configuration of the fiducials. The blue dots are fiducials, the red dot is the origin, which is the target point and the arrows are the eigenvectors of the fiducial point cloud multiplied with their related eigenvalues. (b) Same configuration but moved to match principal axes (eigenvectors) and standard coordinate system. (c) Yz- view of the 3D plot, with distances from first principal axis to each fiducial and target point. f_1 can then be calculated with formula 2.

Formula 1 is used throughout this paper to quantify the error on the target point for different configurations of fiducials. M. Fitzpatrick et al. [1] declares the first part of formula 1 as the translational part, while the second part is the rotational part. This naming is chosen because if d_k is zero for every k, only a translational error occurs.

2 OPTIMISATION OF FIDUCIAL POSITIONING: SENSITIVITY ANALYSIS

In this section, different parameters are altered, while the target registration error is calculated with usage of simulations and with formula 1. It is important to remark that the square of formula 1 gives the rms of the TRE's which is not the same as the mean error on the target point. The rms value for positive arrays is always bigger than the mean value due to the major importance of the biggest values. So:

$$rms(TRE) = \sqrt{\langle TRE^2 \rangle} > \langle TRE \rangle = mean(TRE) \tag{3}$$

T.Chai and R. R. Draxler [2] state that the root mean square error (RMSE) is better to use when the error is normally distributed. Moreover, the fact that outliers will result in too much squatter in the result is proven to be surpressed if the number of different TRE's is big enough. In the case of optical tracking, this method is followed because a big error is totally not accepted. Therefore the rms will result in higher values if there are big or many outliers in the error.

Besides this analytical method, a simulation of the errors can also be performed. Therefore point clouds around each fiducial are created with equally and normally distributed x-, y- and z-coordinates, which are representative of the error that occurs during tracking of the fiducials. By taking a random set of these slightly incorrect points, a representative point for the target can be calculated with transformation using the single value decomposition method as derived by O. Sorkine-Hornung and M. Rabinovich [3]. As such the TRE is obtained, which is then repeated for a large amount of datasets. The mean value or the RMS can then be calculated.

2.1 Triangularity

The first parameter is the triangularity (δ), defined in planar shapes as the shortest distance from one cornerpoint to the opposing side, divided by the length of that opposite side (see figure 4.a). This value can vary from 0 – for a collinear configuration – to $\sqrt{3}/2$ for an equilateral triangle. To see what the influence is on the target registration error, two fiducials are kept in a constant position in space, while the third one is placed in subsequent positions with increasing δ. The rms-value of the TRE divided by rms(FLE) is then plotted relative to δ. To have more insight in the influence of this parameter, some different cases have to be considered.

The first case is with fiducials at:

$$\begin{bmatrix} \{x\} \\ \{y\} \\ \{z\} \end{bmatrix}_{fiducials\ 1,2,3} = \begin{bmatrix} 0 & 0 \xrightarrow[9\,steps]{} \left(\frac{\sqrt{3}}{2} \cdot 200\right) & 0 \\ 0 & 0 & 0 \\ 100 & 200 & 300 \end{bmatrix} \tag{4}$$

The starting point in this configuration is where not only the fiducials are collinear but also the target point is on the same straight line. If formula 1 is considered, it can be seen that d_1 is zero in this case and rotating around the straight line through the three fiducials does not introduce an extra error. As such, there is not that much difference in the error of the target towards the collinear position, which can be seen in figure 4.b. The lower error for bigger triangularity is in fact a result of the more widespread placement of the fiducials, which is explained into more detail later on. The plots are given with logarithmic x-coordinates.

In the second case to find the influence of the triangularity, the fiducials are placed as follows:

$$\begin{bmatrix} \{x\} \\ \{y\} \\ \{z\} \end{bmatrix}_{fiducials\ 1,2,3} = \begin{bmatrix} 30 & 30 \xrightarrow[9\,steps]{} \left(30 + \frac{\sqrt{3}}{2} \cdot 200\right) & 30 \\ 0 & 0 & 0 \\ 100 & 200 & 300 \end{bmatrix} \tag{5}$$

It can be seen as result in figure 4.c that for really small δ, the error is going to very high values. If not zoomed in, the error at collinear fiducials is with formula 1 equal to infinity due to the zero f_1. However for the simulation, this value is equal to 235. This really big error is due to the fact that the sense of rotation is totally gone, and the target point can be turned around the axes [30, 0, z]. Of course this has to be avoided and as such, it can be stated that collinearity is always a problem, because it is difficult to make sure that the target point is exactly positioned. Remark that also here logarithmic x-coordinates are used.

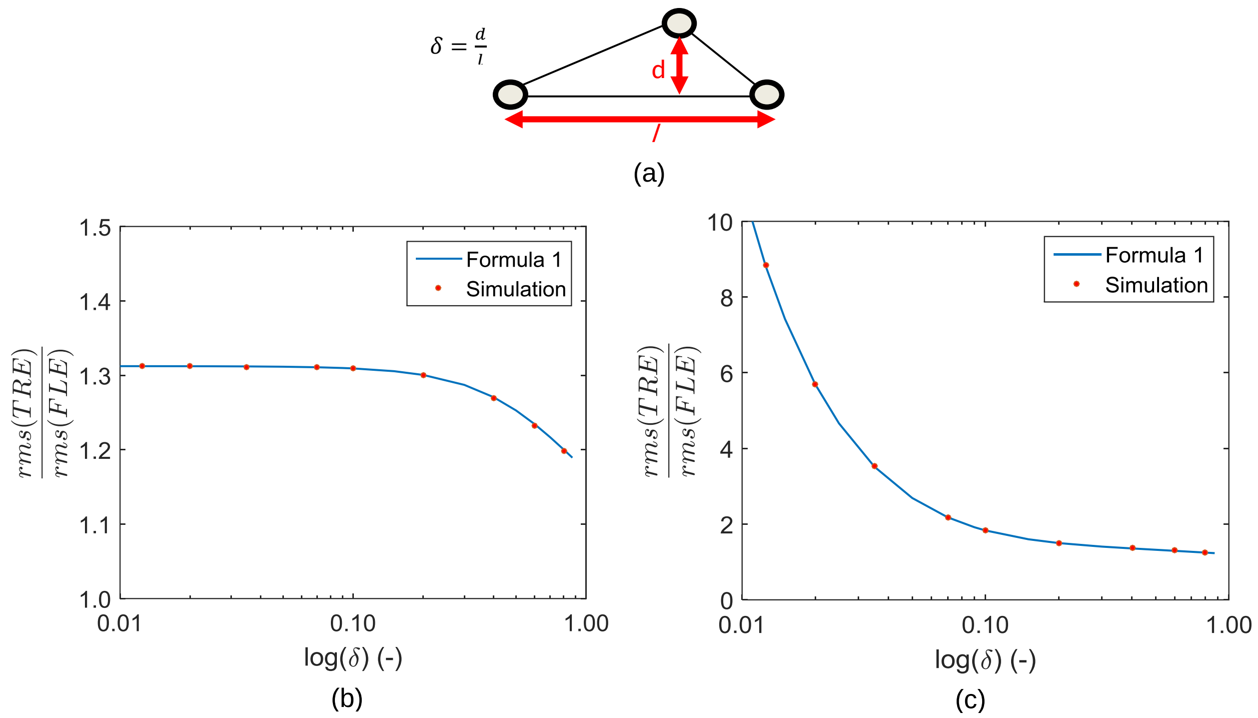

Figure 4: Influence of triangularity on TRE. (a) Definition of triangularity. (b) Starting from collinear fiducials and target point. (c) Starting from collinear fiducials and target point at 30 mm distance.

The red dots in figure 4 are results of the simulations while the blue curve is formula 1. The number of points for each simulation is chose as 10,000. Because the relative error of the simulation compared to the formula is less than 0.1 % with this amount of points, the correctness of the formula for this case is proven.

2.2 Amount of fiducials

An increasing amount of fiducials will lead to an improvement in the error distribution. This can be seen in formula 1 because of the N in the denominator. However, the positioning of the different fiducials also has influence and as such, the factor of decreasing error is difficult to predict. One case is easy to calculate, namely the one where the target point lays in the centre of the fiducials. Then d_i for *i = {1,2,3}* is zero and the formula 1 indicates that the error is proportional to $1/\sqrt{N}$. This is indeed correct as given in figure 5. In this test, the fiducials are placed on a regular polygon around the origin, with {3,4,5,6,7} sides. The distance to the target point is chosen as 1 for each fiducial. This result is similar to the one in the paper of J.B. West* and C. R. Maurer [4].

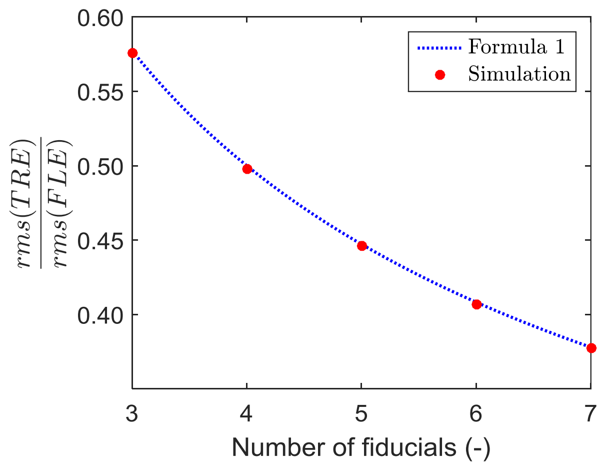

Figure 5: Relative error with respect to number of fiducials, when fiducials are placed in regular polygon

2.3 Widespread of fiducials and distance target point to principal origin of fiducials

There are still two parameters that need to be discussed: d_k and f_k. Both are part of the rotation formula of formula 1. It is the aim here to see how d_k and f_i are changing for different configurations. If first f_k is kept constant - this is the point cloud of fiducials is constant -, and the relative position of the target point to the centre of the fiducial point cloud is changing, the d_k will change. It is important to remark that the f_k's are increasing for increasing *k*. The reason is that f_1 is the rms distance to the first principle axis. The variation of the fiducials is the biggest in that direction and as such the distance to this axis is the smallest. The same can be said for *i = {2,3}* and as such following equation is obtained:

$$f_1 < f_2 < f_3 \tag{6}$$

It is of course clear from formula 1 and formula 6 that also d_k has to decrease for smaller *k* to have the best combination of $d_k's$ and f_k's. As such, the best position of the target point is on the first principal axis of the fiducial cloud. Then the two other distances, d_2 and d_3, will be the same.

The second case is where the distance from the target point and the centre of the fiducials is constant, but the positioning of the different fiducials is changing. Some of the possibilities are blowing up the coordinates from the centre or putting them more in one or another direction. The *f*'s have to be as big as possible because they are in the denominator of formula 1. A test is done in which only the z coordinates are placed more widespread. This ensures that f_2 and f_3 are rising while f_1 stays constant. One expects then a lowering error on the target point, which is indeed reached as can be seen in figure 6. The positions of the fiducials are as follows:

$$\begin{bmatrix} \{x\} \\ \{y\} \\ \{z\} \end{bmatrix}_{fiducials} = \begin{bmatrix} 10 & -10 & 70 & -70 & 10 & -10 \\ 0 & 0 & 0 & 0 & 0 & 0 \\ 120 & 120 & 150 & 150 & 250 & 250 \end{bmatrix} \xrightarrow[5\ equal\ steps]{} \begin{bmatrix} 10 & -10 & 70 & -70 & 10 & -10 \\ 0 & 0 & 0 & 0 & 0 & 0 \\ 35 & 35 & 113 & 113 & 373 & 373 \end{bmatrix} \tag{7}$$

To see what happens with the *d* and *f*-values, they are listed for the smallest and biggest size:

$$\begin{cases} d_{smallest} = [0 \quad 0.1733 \quad 0.1733] \\ f_{smallest} = [0.0412 \quad 0.0556 \quad 0.0692] \end{cases} \rightarrow \begin{cases} d_{smallest} = [0 \quad 0.1733 \quad 0.1733] \\ f_{smallest} = [0.0412 \quad 0.1445 \quad 0.1503] \end{cases} \tag{8}$$

These values are indeed like expected, because the only things that are changing are the last two *f*-values. From formula 1, it can then be seen that the error is indeed lowering.

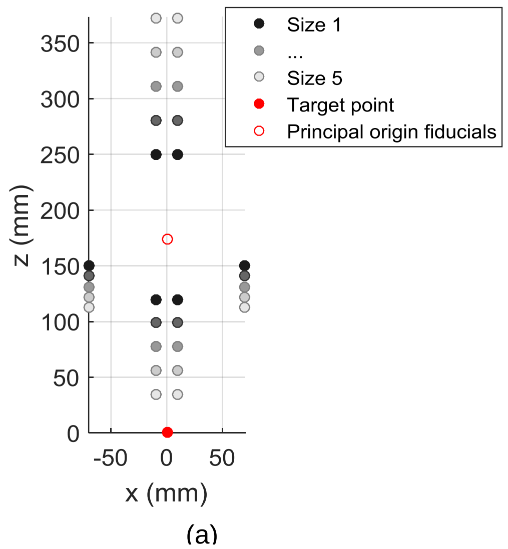

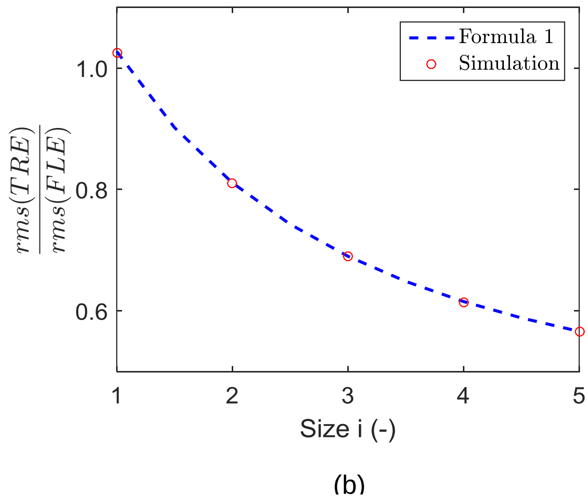

Figure 6: Widespread of the z-coordinate of the fiducials, with constant center of the fiducial cloud. (a) Sketch of the configuration for size 1 to size 5. (b) TRE divided by FLE for the different sizes. Formula 1 is plotted as well as the simulation (red dots).

3 ANALYSIS OF OPTIMAL DESIGN IN 3D AND 2D

3.1 Optimal design

For the parameters described in the previous paragraph, the influence is studied and the optimal values can be chosen. However, to get a new design, a combination of these parameters has to be picked to obtain the smallest error. Therefore, some values need to be fixed, while other need to be optimised. The number of fiducials will be fixed at six. This is a compromise between adding more fiducials to decrease the error and the fact that tracking more than six fiducials can become complicated because of the compact placement in that case. Also occlusions can occur when fiducials are hidden behind each other.

Some things that then still need to be investigated are:

- Is it useful to put the fiducials in a 3D configuration, or does one plane suffices?
- Is it useful to have a large second principal component f_2 or can the solution be almost collinear?
- What is the best first principal axis distribution of fiducials, most fiducials close to the target point, or most far away?

To solve these questions, a Matlab tool is used, namely the Global Optimization Toolbox [5]. The problem is that no solver exists that will yield the global minimum of the function. The most used method is therefore to use a solver which does find a local minimum and to let the solver start at different starting points. There is no certainty of finding the real minimum, but this together with common sense can give us the best solution. The used optimisation algorithm is MultiStart, with 100 different starting positions. Because this algorithm can only work with a few solvers, the fmincon solver is used. However this is good to find fast solutions, but to encounter the best solution, a second solver - with as starting position the result of the first run - needs to be used. Therefore patternsearch is selected. The total workflow of the used method is also drawn in a flowchart:

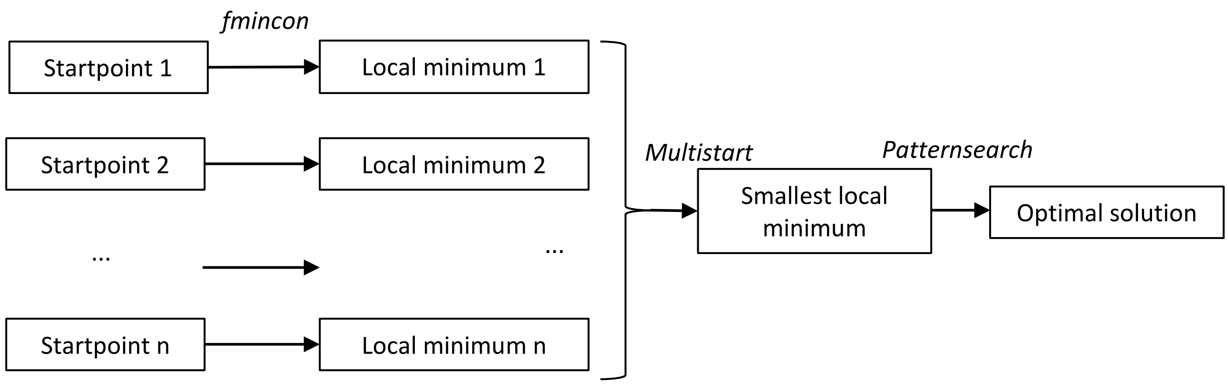

Figure 7: Flowchart of the optimisation function in Matlab

Some bound on the fiducial coordinates have to be stated because otherwise the size would increase to unacceptable values. The most important ones are given below, while all the boundaries are shown in figure 8.

$$\begin{cases} x_{min} = 2 \text{ times } 90 \ \& \ 4 \text{ times } 110\ mm \\ y_{min} = -40\ mm \\ z_{min} = -40\ mm \end{cases} \qquad \begin{cases} x_{max} = 320\ mm \\ y_{max} = 40\ mm \\ z_{max} = 40\ mm \end{cases} \tag{10}$$

The x-coordinates are aligned with the first principal axis, while the y- and z-coordinates are the second and third principal axis components. The fact that only two of x-coordinates of the lower bound are allowed to be 90 mm, while the other ones are put at 110, is because otherwise the algorithm would put 4 or 5 fiducials at this distance, which is of course practically not possible because of the small allowed distance there. In figure 8 the front and back of the allowed volume is put at a pyramid wise tip to avoid widespread fiducials at close positions.

The volume and the solution (red dots) are pictured in figure 8. The coordinates of the result are:

$$\text{Result}_{3D} = \begin{bmatrix} 90 & 90 & 110 & 110 & 110 & 320 \\ -20 & -20 & 40 & -40 & 40 & -11.75 \\ 0 & 0 & -33.33 & -33.33 & 33.33 & 0 \end{bmatrix} (mm) \tag{11}$$

Other important parameters of the result are:

$$\begin{cases} rms\ (TRE)/rms\ (FLE) = 0.6677 \\ d_k = [9.48 \quad 138.46 \quad 138.13]\ (mm) \\ f_k = [32.28 \quad 84.39 \quad 87.91]\ (mm) \end{cases} \tag{12}$$

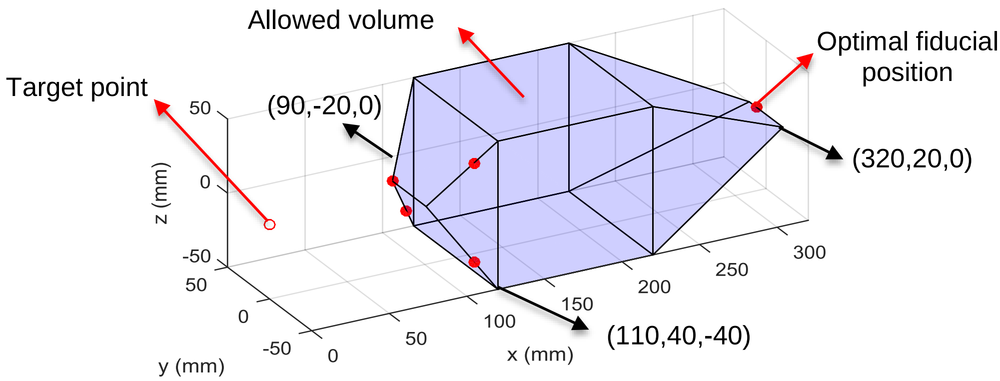

Figure 8: Allowed volume and optimal solution for the fiducials when a 3D configuration is used.

Some problems arise with this 3D configuration when the practical side of the design is encountered. Fiducials one and two are at the same spot, fiducials three and five are above each other and linkages to fix the fiducials will reduce other fiducials' visibility. Therefore, one can look to 2D and see what the loss in TRE is.

The volume is now a xy-projection of the 3D volume. This volume and the solution obtained with the optimisation algorithm of figure 7 are pictured in figure 9 (red dots). The coordinates of the result are:

$$\text{Result}_{3D} = \begin{bmatrix} 90 & 90 & 110 & 110 & 320 & 320 \\ -20 & 20 & 40 & -40 & 20 & -20 \\ 0 & 0 & 0 & 0 & 0 & 0 \end{bmatrix} (mm) \tag{13}$$

Other important parameters of the result are:

$$\begin{cases} rms\ (TRE)/rms\ (FLE) = 0.6737 \\ d_k = [0 \quad 173.33 \quad 173.33]\ (mm) \\ f_k = [28.28 \quad 104.03 \quad 107.80]\ (mm) \end{cases} \tag{14}$$

The optimal solution is now known in one plane and because the error is not that much bigger than the 3D case, it is opted to choose this one.

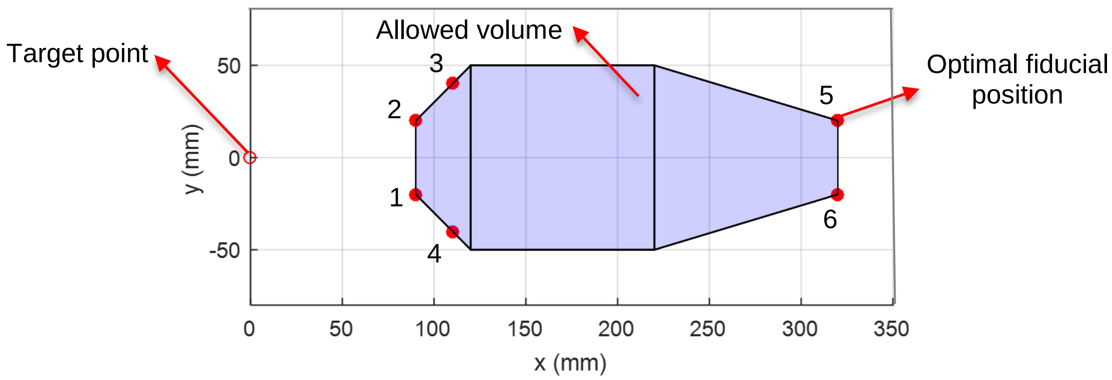

Figure 9: Allowed space and optimal solution for the fiducials for a 2D configuration

3.2 Robustness and evaluation of design

To check the robustness of the design parameters, some important sizes can still be changed to increase the precision of the probe. This is: the boundaries that are given in optimisation function can be changed, while the positioning is kept constant. Some simulation results are given below:

Table 1: Influence on the error of changing parameters in the mechanical design of the pointer

Changed parameter	Value (from → to) (mm)	rms (TRE) / rms (FLE)	% decrease
$x_{fiducial\ 5,6}$	$320 \rightarrow 330$	0.66	-1.53
$y_{fiducial\ 5,6}$	$\lvert 20\rvert \rightarrow \lvert 30\rvert$	0.67	-0.34
$y_{fiducial\ 3,4}$	$\lvert 40\rvert \rightarrow \lvert 50\rvert$	0.67	-0.49
$x_{fiducial\ 1,2}$	$90 \rightarrow 80$	0.65	-2.82
$z_{fiducial\ 1,2,3,4,5,6}$	$0 \rightarrow 10$	10.05	1435.21

That the last row of the table gives such big errors, is due to the fact that the matching algorithm cannot orientate the solution, because of its symmetry. Therefore, some adjustment need to be done to make the shape asymmetrically. This is reached by placing fiducial 4 from $y = -40$ to $y = -50$.

Sometimes the cameras can not see every fiducial, because some of them are occluded. Therefore the simulation is now done with a lower amount of fiducials. The results are given in following table:

Table 2: Influence on error when one or more fiducials are occluded.

fiducials occluded	rms (TRE) / rms (FLE)	% increase of error
1 or 2	0.77	15.05
3	0.77	14.19
4	0.76	13.63
5 or 6	0.73	7.66
1 and 2	0.94	39.90
3 and 4	0.87	28.71
5 and 6	2.80	415.96
1 and 6	0.82	22.25

When only one fiducial is occluded, there is not a really big increase in TRE, while for 2 occluded fiducials, there can arise big problems. This case needs to be avoided.

A third way to see what the robustness is, can be done by not only calculating the rms of the TRE, but by plotting the whole distribution of the TRE compared to the distribution of FLE. It can be seen in figure 10 that the TRE distribution has a smaller mean value, as calculated during the optimisation process. It is also beneficial that the distribution of the TRE expires faster than the one for the FLE, this is required to avoid really large errors at some points.

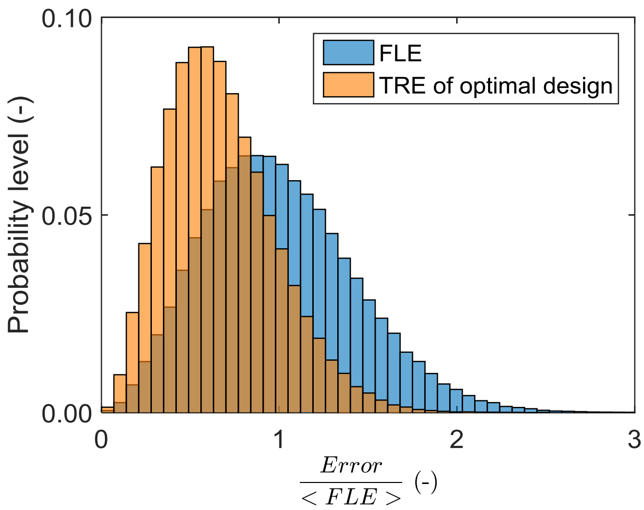

Figure 10: FLE and TRE distributions of the optimal design

3.3 Practical evaluation of the design

The optimised mechanical pointer is tested with an optical tracking system (six cameras type Flex 13: © 2017 NaturalPoint, Inc. DBA OptiTrack [6]). To compare the practical results with the simulations, the same parameters are tested as in figure 10, but now with real measurements. This is given in figure 11.

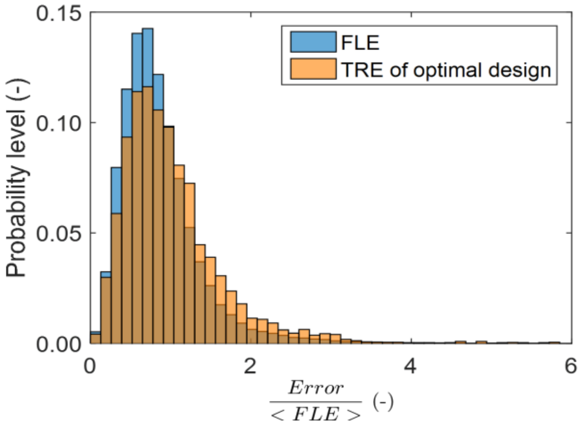

Figure 11: FLE and TRE distributions for the practical design

It is clear that the TRE is in practice bigger than the FLE. The real and relative values are stated below:

$$\begin{cases} rms\ (FLE) = 0.0050\ mm \\ rms\ (TRE) = 0.0059\ mm \end{cases} \rightarrow \frac{rms\ (TRE)}{rms\ (FLE} = 1.18 \tag{15}$$

The rms of the FLE in this case is the mean of the ones for each fiducial. If these are treated separately, following values are obtained, with the number of the fiducial the same as in figure 9:

Table 3: FLE for each fiducial separately, with numbers from figure 9.

Fiducial	1	2	3	4	5	6
FLE (mm)	0.0050	0.0043	0.0045	0.0056	0.0050	0.0052

4 DISCUSSION

To understand the difference between the practical result and the theoretical simulation, the assumptions that were made in the first paragraphs have to be examined. There is one major assumption of the simulation as well as formula 1 which is not fulfilled in practice, namely the normally distributed error around each fiducial. This is due to the limited amount of pixels of the cameras that have a resolution of 1280 ·1024 [6]. As such, the measured position of the fiducial is not normally distributed. This can be seen on figure 12.b, where the yz-view of the measured points are pictured for fiducial 4. When the distribution of the FLE is then plotted, there are two maxima occurring as can be seen in figure 12.a. That all the FLE's are changing for different fiducials is also due to the pixel wise targeting of the midpoint of the spherical fiducials.

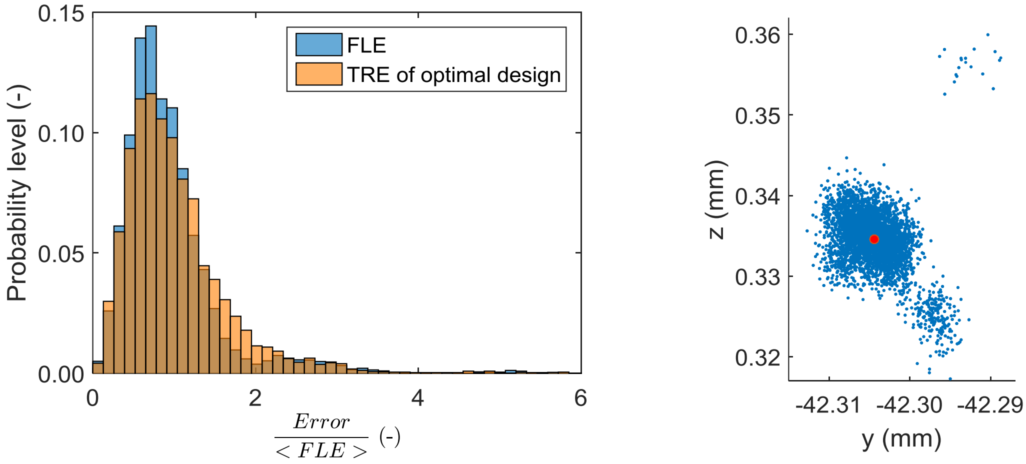

(a) (b)

Figure 12: Error on one specific fiducial (Number 4). (a) TRE distribution of the target compared to the FLE distribution of one fiducial. This FLE has two maxima because of the non-normally distributed coordinates. (b) Y-z projected view of the measured points for fiducial 4.

5 CONCLUSIONS

The results of the practical design, with a target registration error almost equal to the fiducial localisation error, shows that optimisation indeed gives a well acting pointer. The formula stated in literature [1] as well as simulations lead to a design with six markers, organised close around the first principal axis. Putting the target point on the same axis, results in small errors because rotating errors are minimised. The fact that the practical design is a bit less performing than the simulations is explained by the non-normally distributed x-, y- and z-values of the fiducials measurements. Because this behaviour is inevitable and independent of the design, the optimisation process keeps its value.

6 NOMENCLATURE

FLE	Fiducial Localisation Error	mm
FRE	Fiducial Registration Error	mm
TRE	Target Registration Error	mm
Rms	Root mean square	-

7 ACKNOWLEDGEMENTS

8 REFERENCES

[1] J.M. Fitzpatrick, J. B. West and C.R. Maurer, Predicting error in rigid-body, point-based registration., IEEE transactions on medical imaging, 17 (5), 1998

[2] T. Chai and R.R. Draxler, Root mean square error (RMSE) or mean absolute error (MAE)? – Arguments against avoiding RMSE in the literature. Geoscientific model development, 2014

[3] O. Sorkine-Hornung and M. Rabinovich, Leas-Squares Rigid Motion Using SVD, department of computer science, Zurich, 2017.

[4] J.B. West* and C. R. Maurer. Designing optically tracked instruments for image-guided surgery. IEEE transactions on medical imaging, 23 (5): 533-546, 2004.

[5] Solve multiple maxima, multiple minima, and nonsmooth optimization problems [Internet]. [8 April 2016]. Available from : https://nl.mathworks.com/products/global-optimization.html

[6] A medium volume motion capture camera with excellent precision. [Internet]. [5 April 2016]. Available from: http://www.optitrack.com/products/flex-13/specs.html